Reduced NPY Y1 receptor hippocampal expression and signs of decreased vagal modulation of heart rate in mice

Reduced NPY Y1 receptor hippocampal expression and signs of decreased vagal modulation of heart rate in mice

Rosario Statello[1], Luca Carnevali[1], Silvia Paterlini[1], Laura Gioiosa[1], Ilaria Bertocchi[2], Carola Eva[2], Paola Palanza[1*], Andrea Sgoifo[1*].

[1] Department of Neuroscience, University of Parma, Italy

[2] Neuroscience Institute Cavalieri-Ottolenghi Foundation, University of Turin, Italy

Corresponding author: Prof. Andrea Sgoifo, Stress Physiology Laboratory, Department of Neuroscience, University of Parma, Parco Area delle Scienze 11/a, 43123 Parma, Italy

Tel: +39 0521 905625; fax: +39 0521 905673

E-mail address: andrea.sgoifo@unipr.it

* These authors contributed equally to this work

Abstract

Central neuropeptide Y (NPY) signaling participates in the regulation of cardiac autonomic outflow, particularly via activation of NPY-Y1 receptors (Y1Rs). However, the specific brain areas and neural pathways involved have not been completely identified yet. Here, we evaluate the role of hippocampal Y1Rs in the modulation of the autonomic control of cardiac function using a conditional knockout mouse model. Radiotelemetric transmitters were implanted in 4-month-old male mice exhibiting reduced forebrain expression (rfb) of the Y1R ($Npy1r^{rfb}$, n=10) and their corresponding controls ($Npy1r^{2lox}$, n=8). ECG signals were recorded (i) during resting conditions, (ii) under selective pharmacological manipulation of cardiac vagal activity, and (iii) during acute and chronic psychosocial stress challenges, and analyzed via time- and frequency-domain analysis of heart rate variability. $Npy1r^{rfb}$ mice showed a lower Npy1r mRNA density in the dentate gyrus and in the CA1 region of the hippocampus. Under resting undisturbed conditions, $Npy1r^{rfb}$ mice exhibited (i) a higher heart rate, (ii) a reduced overall heart rate variability, and (iii) lower values of the indices of vagal modulation compared to $Npy1r^{2lox}$ counterparts. Following pharmacological vagal inhibition, heart rate was higher in control but not in $Npy1r^{rfb}$ mice compared to their respective baseline values, suggesting that tonic vagal influences on heart rate were reduced in $Npy1r^{rfb}$ mice. The magnitude of the heart rate response to an acute psychosocial stressor was smaller in $Npy1r^{rfb}$ mice compared to $Npy1r^{2lox}$ counterparts (likely due to a concurrent lower vagal withdrawal), even though absolute heart rate values did not differ between the two groups. These findings suggest that reduced hippocampal Y1R expression leads to a decrease in resting vagal modulation and heart rate variability, which, in turn, may determine a reduced cardiac autonomic responsiveness to acute stress challenges.

Keywords: NPY; Stress; Heart; Autonomic; knockout; Parasympathetic.

1. Introduction

Neuropeptide Y (NPY) is widely distributed in the central nervous system [1], with particularly high concentrations in the hypothalamus [2] and limbic system [3, 4]. NPY is involved in the regulation of a variety of complex functions that range from food intake to emotional state [5]. These effects are mediated by multiple G-protein coupled receptor subtypes, which are characterized by different tissue localization and pharmacological properties [6-8]. In particular, accumulating evidence suggests that central Y1 receptors (Y1Rs) play a critical role in the inhibition of the sympathetic outflow to peripheral tissues. For example, it has been shown in rats that i.c.v. (lateral ventricle) administration of the Y1R agonist [Leu^{31},Pro^{34}]NPY reduces basal noradrenaline release from the paraventricular nucleus of the hypothalamus (PVN) [9], the major site of autonomic regulation via projections to the rostral ventro-lateral medulla and the spinal cord. Moreover, NPY, acting on Y1Rs, decreases noradrenaline overflow from both the hypothalamus and the medulla in vitro [10]. A recent study has elegantly demonstrated that NPY released from the arcuate nucleus (ARC) suppresses tyrosine hydroxylase (TH) expression in the PVN via activation of Y1Rs [11]. This effect was associated with a reduction in TH expression in the locus coeruleus and other regions (such as the A1/C1 cell groups) in the brain stem [11], which would ultimately lead to a reduced sympathetic outflow to peripheral tissues [11]. Supporting this view, nanoinjection of NPY into the PVN decreases heart rate (HR), sympathetic nerve activity and baroreflex control of HR in anesthetized rats via activation of Y1Rs and Y5Rs [12]. In mice, Tovote and colleagues observed that bilateral i.c.v. injections of NPY dose-dependently induced bradycardia and also blunted the tachycardic response to a fear conditioning challenge [13], the latter via Y1R-mediated inhibition of stress-induced sympathetic activation [13]. Similarly, global knockout of the Y1 receptor gene in mice led to a larger HR activation during social defeat stress [14]. These findings support the view that NPY-Y1R signaling may play an important role also in constraining stress-induced sympathetic activation [15, 16]. While the relationship between NPY-Y1R signaling in the ARC/PVN axis and sympathetic nervous system has been documented, there is little known about the neural pathways and mechanisms that control it. Indeed, in contrast with the above reported observations that are suggestive of a central sympathetic inhibitory role of Y1Rs, global knockout of the NPY-

Y1R gene in mice led to resting bradycardia, which was likely due to a reduced basal sympathetic tone and increased parasympathetic activity [14]. This apparent contradiction might be ascribed to compensatory effects that are due to gene inactivation in early development and/or might underlie different roles played by Y1Rs at different levels in the central autonomic network.

Recently, a conditional knockout mouse model in which the inactivation of the Y1 receptor gene is restricted to excitatory neurons in the hippocampus, in particular when mice were reared by foster mothers exhibiting high levels of maternal care, has been developed [17]. Therefore, this animal model may be useful for understanding the contribution of hippocampal Y1Rs for central autonomic cardiovascular control. In order to reach this goal, autonomic modulation of cardiac function was assessed in the above mentioned conditional knockout mouse model during (i) baseline conditions, (ii) selective pharmacological autonomic manipulations, and (iii) acute and chronic psychosocial stress challenges, via time- and frequency-domain analysis of HR variability (HRV).

2. Methods

2.1. Animals, housing conditions and ethics statements

Experiments were performed on 4-month-old male conditional knockout mice ($Npy1r^{rfb}$, n=10) and their control littermates ($Npy1r^{2lox}$, n=8) that were matched for body weight. $Npy1r^{rfb}$ and $Npy1r^{2lox}$ mice (background strain: C57BL/6J) were generated following the breeding scheme described by Bertocchi et al. (see [17] for details). Briefly, $Npy1r^{2lox}/Tg^{\alpha CamKII\text{-}tTA/LC1}$ mice (named herein $Npy1r^{rfb}$) were generated using doxycycline dependent control of the Cre-LoxP system. Using this approach, Bertocchi et al. [17] achieved the deletion of Npy1r in the hippocampal CA1 and CA3 pyramidal and in the dentate gyrus granule cell layers. Since the phenotype of $Npy1r^{rfb}$ mutants becomes evident only in males reared by foster mothers showing high level of maternal cares versus adopted pups, immediately after birth the $Npy1r^{rfb}$ male mice used in our study were fostered to Dox-naive CD1 dams, which display high levels of maternal cares (unpublished data). Littermates comprising $Npy1r^{2lox}/Tg^{\alpha CamKII\text{-}tTA}$, $Npy1^{r2lox}/Tg^{LC1}$, and $Npy1r^{2lox}$ genotypes were used as controls (named herein $Npy1r^{2lox}$ controls), as in Bertocchi et al. [17]. After weaning, mice were kept in same sex sibling groups in 40x20x20 cages in rooms with humidity- (50 ± 10%) and temperature- (22 ± 2 °C) controlled conditions, with food and water available ad libitum. Experiments were performed during the light phase of the 12-h light/dark cycle (lights on at 7 a.m.). All experimental procedures and protocols were approved by the Veterinarian Animal Care and Use Committee of Parma University and conducted in accordance with the European Community Council Directives of 22 September 2010 (2010/63/UE).

2.2. Transmitter implantation and radiotelemetry system

ECG (sampling frequency 2 KHz), body temperature (T, °C) and locomotor activity (LOC, counts per minute, cpm) signals were recorded by a radiotelemetry system. It consisted of transmitters (TA10ETA-F20, Data Sciences Int., St.Paul, MN, USA) and platform receivers (RPC-1, Data Science Int., St.Paul, MN, USA), which were connected to a computer containing Art-Gold 1.10 data acquisition system (Data Science Int., St.Paul, MN, USA). Transmitter implantation was performed under isoflurane anesthesia (2% in 100% oxygen), as previously described [18]. The

transmitter's body was implanted intraperitoneally and two electrodes (wire loops) were fixed to the dorsal surface of the xyphoid process and in the anterior mediastinum close to the right atrium, respectively. This surgical procedure guarantees high quality ECG recordings, even during sustained physical activity. After surgery, mice were individually housed, injected with Gentamicin sulphate (Aagent, Fatro, 1ml/kg, S.C.) and allowed two weeks of recovery before the beginning of the experimental recordings.

2.3. General experimental outline

The timeline of the experimental protocol is depicted in Figure 1. Specific experimental procedures and data analysis are described in the following sections. After recovery from surgery, mice were weighed and left undisturbed in their home cages for 6 days (days 1-6). On days 7 and 9, they underwent pharmacological autonomic challenges. From day 12 to day 25, mice were housed in the cage of a dominant mouse in order to mimic a chronic psychosocial stress condition. At the end of the experimental protocol, mice were sacrificed by decapitation. Brains were rapidly removed and immediately frozen in liquid nitrogen, then stored at -80° C until analysis.

2.4. Daily rhythms of HR, HRV, T and LOC

ECG, T and LOC signals were sampled around-the-clock for 2 min every 30 min in baseline conditions (Basal Rhythms, days 1-6) and during chronic psychosocial stress (Stress Rhythms 1, days 16-19; Stress Rhythms 2, days 22-25) (Fig. 1). Heart rate (HR, beats per minute, bpm), HRV parameters (see ECG analysis section for details), T and LOC were calculated as mean values of the 12-h light and 12-h dark phases of the daily cycle for each recording day. Subsequently, they were further averaged as mean values of the light and dark phase for each recording period.

2.5. Pharmacological autonomic challenge

On day 7 and 9 (Fig. 1), mice were intraperitoneally injected with either i) vehicle (0.9% NaCl, 1 ml/kg) or ii) methylscopolamine (muscarinic receptor antagonist, 0.1 mg/kg), with a rotational

151 design. Continuous ECG recordings were performed prior to (for 30 min, baseline condition) and
152 following (for 60 min) each injection, with the mice in their home cages.
153
154 2.6. Chronic psychosocial stress
155 In the present study we applied a modified version of the standard chronic psychosocial stress
156 paradigm [18, 19], which is based on the classical resident-intruder test [20]. Six-month-old CD1
157 mice were housed with a female partner for 1 week and then individually housed and trained to
158 aggressively defend their territory from same sex mice intruders that were younger and lighter.
159 These dominant animals served as residents. Each experimental mouse was introduced as an
160 intruder in the home cage of a resident male; once there, it was attacked and subordinated by the
161 resident mouse (social defeat). After 10 min, the two animals were separated by a perforated
162 polystyrene-metal partition that divided the cage into two equal-area sections. Thus, the intruder
163 mouse was protected from direct physical contact but it was in constant olfactory, auditory and
164 visual contact with the resident (psychosocial challenge). The partition was removed five times
165 during the experimental protocol (Fig. 1) at an unpredictable time between 9:00 and 13:00 h and
166 repositioned after 2 min to prevent injuries. After each interaction, the experimental mice were
167 closely inspected for any improper injury and were excluded from further procedures in case they
168 were wounded. During the first episode of agonistic interaction, continuous ECG recordings were
169 performed for 30 min in baseline conditions (with the mice in their home cage), during the 10-min
170 agonistic interaction, and for 60 min after the intruders were again separated from the residents by
171 the partition.
172
173 2.7. Heart rate variability (HRV) analysis
174 HRV analysis was carried out on ECG recordings using ChartPro 5.0 software (ADInstrument,
175 Sydney, Australia), based on the recommendations for HRV analysis in mice [21]. Initially, each
176 ECG recording was split in 2-min temporal segments (0-2 min; 2-4 min; etc.). Ectopic beats and
177 recording artifacts were then removed following visual inspection of unprocessed ECG signals.
178 Subsequently, HR and time- and frequency-domain parameters of HRV were quantified for each 2-

min time period. In the time domain, the root mean square of successive R-R interval differences (RMSSD, ms) was quantified; this index reflects short-term, high-frequency variations of RR interval, which are mainly due to cardiac parasympathetic activity [22]. In the frequency-domain, the power spectrum was obtained with a fast Fourier transform-based method (Welch's periodogram: 256 points, 50% overlap, and Hamming window). The following parameters were evaluated: i) the total power of the spectrum (ms^2), which reflects all the cyclic components responsible for variability [23], and ii) the power (ms^2) of the high frequency band (HF, 1.5-5.0 Hz), which reflects the activity of the parasympathetic nervous system and is related to respiratory sinus arrhythmia [24].

2.8. In Situ Hybridization for Npy1r mRNA

In situ hybridization was performed on 14-µm-thick coronal brain sections, according to the protocol reported by Wisden and Morris [25], in $Npy1r^{rfb}$ (n=4) and $Npy1r^{2lox}$ (n=4) mice. Four different 40-/45-mer oligonucleotide S35-labeled probes were simultaneously used to increase the signal and the reaction was carried out as previously described [17]. The area of interest of clearly distinguishable nuclei was defined following the boundaries of the labeled regions [dentate gyrus granule cell layer (DG)], whereas three to four spots were used for each slice in poorly contrasted regions [CA1 pyramidal cell layer (CA1) and CA3 pyramidal cell layer (CA3)]. Optical densities (OD unit) were measured and averaged after a rodboard calibration. Background was measured by averaging three to five spots in the surrounding blank region of the autoradiogram, then subtracted from the corresponding nucleus value.

.

2.9. Statistical analysis

All statistical analyses were performed using the software package SPSS (version 22). Two-way ANOVA for repeated measures with "group" as between-subject factor (2 levels: $Npy1r^{rfb}$ and $Npy1r^{2lox}$) was applied for ECG and telemetric data obtained from: i) baseline around-the-clock recordings, with "time" as within-subject factor (6 levels: day 1, 2, 3, 4, 5 and 6); ii) pharmacological challenges, with "time" as within-subject factor (4 levels: baseline; post injection 1, 2, 3); iii) first

episode of social defeat, with “time” as within-subject factor (8 levels: baseline, fight, sensory contact 1, 2, 3, 4, 5 and 6); iv) around-the-clock recordings during chronic social stress, with “time” as within-subject factor (3 levels: baseline, stress 1 and stress 2). Follow-up analyses were conducted using Student’s “t” tests, with a Bonferroni correction for multiple comparisons for each outcome variable separately. Statistical significance was set at $p<0.05$.

3. Results

3.1. Body weight

Prior to surgery, body weight was 25.0±0.9 g for Npy1r^{rfb} mice and 26.0±1.2 g for Npy1r^{2lox} mice (n.s.). No significant differences between the two groups were found in body weight at the beginning of the experimental protocol (day 1) (Npy1r^{rfb}: 26.3±0.3 g vs. Npy1r^{2lox} 27.2±0.8 g).

3.2. Expression of Npy1r mRNA in the hippocampus of control and conditional mutants

In Npy1r^{rfb} mice, Npy1r mRNA expression was significantly lower in hippocampal CA1 pyramidal cell layers ($t=-3.1$, $p<0.05$) and in dentate gyrus granule cell layers ($t=-3.4$, $p<0.05$) compared with their control littermates, whereas no difference was observed in CA3 pyramidal cell layers between the two groups (Fig. 2).

3.3. Daily rhythms of HR, HRV, T and LOC during baseline conditions

The daily rhythms of HR, HRV indices, T and LOC in resting conditions are depicted in Figure 3 and summarized in Table 1. Two-way ANOVA yielded a main effect of "group" for HR ($F=20.1$, $p<0.01$), total power ($F=7.0$, $p<0.05$), RMSSD ($F=5.3$, $p<0.05$), and HF ($F=4.6$, $p<0.05$) values. Follow-up analyses revealed that Npy1r^{rfb} mice had significantly higher HR values than Npy1r^{2lox} mice during both the light ($t=2.9$, $p<0.05$) and dark ($t=3.9$, $p<0.01$) phases of the daily cycle (Fig. 3A and Table 1). Npy1r^{rfb} mice exhibited significantly lower values of total power than Npy1r^{2lox} mice during both the light ($t=2.6$, $p<0.05$) and the dark ($t=3.0$, $p<0.01$) phases of the light-dark cycle (Fig. 3B and Table 1). RMSSD values also resulted significantly lower in Npy1r^{rfb} mice than Npy1r^{2lox} counterparts in both phases (light: $t=2.4$, $p<0.05$; dark: $t=2.5$, $p<0.05$) (Fig. 3C and Table 1). Also spectral power values in the HF band were lower in Npy1r^{rfb} compared to Npy1r^{2lox} mice (light: $t=2.4$, $p<0.05$; dark: $t=1.9$, $p=0.07$) (Fig. 3D and Table 1). In addition, Npy1r^{rfb} mice had significantly higher T values than Npy1r^{2lox} mice during the light phase ($t=2.0$, $p=0.05$) (Fig. 3E and Table 1). Lastly, no significant differences between the two groups were observed for LOC values (Fig. 3F and Table 1).

241

242 3.4. Cardiac autonomic response to the pharmacological autonomic manipulation

243 Cardiac autonomic responses to vehicle or methylscopolamine injection are depicted in Figure 4.

244 Before vehicle injection, HR was significantly higher in Npy1r^{rfb} than in Npy1r^{2lox} mice (t=2.6,

245 p<0.05) (Fig. 4A). In the same period, HRV analysis revealed that Npy1r^{rfb} mice had significantly

246 lower values of RMSSD (t=2.1, p=0.05) and HF spectral power (t=2.2, p<0.05) compared to

247 Npy1r^{2lox} mice (Fig. 4C, E). The injection of vehicle provoked an increase in HR and a reduction in

248 RMSSD and HF values in both groups, with no group differences in the mean values of these

249 parameters (Fig. 4A, C, E). All parameters returned to baseline values within 40 min. During the

250 last 20-min recording period (min 40-60), mean HR was significantly higher in Npy1r^{rfb} compared to

251 Npy1r^{2lox} mice (t=2.2, p<0.05) (Fig. 4A). In the same period, RMSSD and HF mean values were

252 lower in Npy1r^{rfb} than in Npy1r^{2lox} mice (RMSSD: t=2.0, p=0.06; HF: t=2.6, p<0.05) (Fig. 4C, E).

253 Before methylscopolamine injection, HR was significantly higher in Npy1r^{rfb} compared to Npy1r^{2lox}

254 mice (t=2.3, p<0.05). Blockade of muscarinic receptors with methylscopolamine provoked a

255 significant reduction of RMSSD (Npy1r^{rfb}: t=8.5, p<0.01; Npy1r^{2lox}: t=6.5, p<0.01) and HF (Npy1r^{rfb}:

256 t=5.4, p<0.01; Npy1r^{2lox}: t=4.1, p<0.01) values in both groups that persisted through the 60-min

257 recording period (Fig. 4D, F). There were no differences in the peak HR response to

258 methylscopolamine injection between the two groups (Fig. 4B). However, contrary to what has

259 been observed during vehicle (control) condition, during the last 20-min recording period (min 40-

260 60) mean HR was (i) similar between the two groups, and (ii) significantly higher in Npy1r^{2lox}

261 compared to the respective baseline value (t=2.2, p<0.05).

262

263 3.5. HR, HRV, and LOC response to the first episode of social defeat

264 Cardiac autonomic and LOC responses to the first episode of social defeat are depicted in Figure

265 5. Two-way ANOVA yielded a significant effect of time for HR (F=18.9, p<0.01) and LOC (F=4.4,

266 p<0.05) values. In baseline conditions, HR was significantly higher in Npy1r^{rfb} than in Npy1r^{2lox}

267 mice (t=2.2, p<0.05) (Fig. 5A). No differences in absolute values of HR were observed between the

268 two groups during the 10-min fight period and the following 60-min sensory contact phase (Fig.

5A). However, the magnitude of the HR response during the 10-min fight period (delta values) was significantly smaller in $Npy1r^{rfb}$ than in $Npy1r^{2lox}$ mice ($t=-4.6$, $p<0.01$) (Fig. 5B). Consistently, in baseline conditions $Npy1r^{rfb}$ mice had significantly lower HF spectral power values compared with $Npy1r^{2lox}$ mice ($t=2.5$, $p<0.05$) (Fig. 5C). During the 10-min fight period, HF absolute values were similar between the two groups (Fig. 5C), with the magnitude of the stress-induced reduction in HF values being significantly smaller in $Npy1r^{rfb}$ than in $Npy1r^{2lox}$ mice ($t=2.5$, $p<0.05$) (Fig. 5D). No differences in LOC values were observed between $Npy1r^{rfb}$ and $Npy1r^{2lox}$ mice in baseline conditions and in response to the social challenge (Fig. 5E, F).

3.6. Daily rhythms of HR, HRV, T and LOC during chronic psychosocial stress

HR, HRV, T and LOC values during the light and dark phases of the chronic psychosocial stress period are summarized in Table1. Two-way ANOVA revealed that chronic exposure to psychosocial stress led to (i) higher HR values ($F_{light}=20.0$, $p<0.01$; $F_{dark}=19.8$, $p<0.01$), and (ii) lower RMSSD ($F_{light}=4.9$, $p<0.05$), total power ($F_{dark}=7.2$, $p<0.05$) and HF ($F_{light}=6.7$, $p<0.05$) values compared to baseline conditions (Table 1). However, there were no differences between the two groups in HR, HRV parameters, T and LOC during both stress rhythm 1 and stress rhythm 2 periods (Table 1).

4. Discussion

This study demonstrates that reduced expression of hippocampal Y1Rs in mice is associated with an increase in heart rate and a decrease in vagal neural modulation at rest.

In the present study, HRV analysis was carried out in order to characterize cardiac autonomic neural modulation of Npy1r^{rfb} mice under different experimental conditions. During both the light and the dark phases of the daily cycle, Npy1r^{rfb} mice exhibited a lower cardiac vagal modulation, as indexed by RMSSD and HF, which was likely responsible for the resting tachycardia and reduced overall HRV (total power) observed in these mice. Indeed, such changes could not be ascribed to a different level of somatomotor activity between the two groups. Rather, an important confirmation of the involvement of autonomic mechanisms in determining resting tachycardia in Npy1r^{rfb} mice comes from the pharmacological blockade of muscarinic receptors with methylscopolamine. Under this condition of potent and sustained pharmacological inhibition of cardiac vagal modulation, and after recovery from the stress of injection (see vehicle injection condition for a comparison), the group difference in baseline heart rate was abolished. This was due to the fact that heart rate under pharmacological vagal inhibition was higher in control but not in Npy1r^{rfb} mice compared to their respective baseline values. Consequently, it may be reasonable to hypothesize that tonic vagal influences on heart rate were reduced in Npy1r^{rfb} mice, leading to resting tachycardia. Interestingly, we found that baseline body temperature values were also somewhat higher in Npy1r^{rfb} mice. In rodents, brown adipose tissue (BAT) is the main site of nonshivering thermogenesis, and it is under tight control by the sympathetic nervous system [26]. Therefore, signs of hyperthermia in Npy1r^{rfb} mice might suggest an increased sympathetic drive to BAT.

In this study, Npy1r^{rfb} mice Y1R expression is significantly reduced in the dentate gyrus and the CA1 region of the hippocampus, where Y1Rs have been associated with glutamate-positive and NPY-positive neurons [27]. The ventral CA1 hippocampal field is thought to be linked by multisynaptic connections to the sympathetic-related regions of the hypothalamus, suggesting its possible involvement in a higher-brain autonomic circuit [28]. In addition, the hippocampus

connects to nucleus tractus solitarius-projecting regions of the medial prefrontal cortex (mPFC), such as the infralimbic cortex [29], indicating that hippocampal actions on autonomic function may also be routed through the mPFC. Importantly, electrical and chemical stimulation of the hippocampal formation in the anesthetized and the awake rat decreases heart rate, blood pressure and respiratory rate [30, 31]. Interestingly, pharmacological manipulation of vagal activity with methylatropine revealed that the cardiovascular, but not the respiratory, responses were mediated partially by vagal influences and partially by sympathetic influences [30]. Taken together, these preliminary observations indicate that hippocampal Y1Rs may participate in the control of autonomic outflow to peripheral tissues under baseline, undisturbed conditions. In a previous study, Npy1r^{rfb} mice have been characterized as having reduced body weight, less adipose tissue, and lower serum leptin levels [17]. Here, mice did not differ for body weight, either prior or after surgery recovery, as they were matched to avoid possible bias. Therefore, we might cautiously assume that body weight is not a major determinant of the autonomic phenotype described in Npy1r^{rfb} mice. On the other hand, the hippocampus is an important component of the neuronal circuitry controlling anxiety-related behaviors and Npy1r^{rfb} mice have been previously shown to display higher levels of anxiety in the elevated plus maze and open field tests [17]. These findings are consistent with a previous observation that overexpression of virally-transduced NPY in the mouse hippocampus produces anxiolytic-like effects [32]. Moreover, in humans NPY haploinsufficiency is correlated with trait anxiety [33]. Given that anticipation of future aversive events is a key aspect of anxiety disorders [34] and that anxiety is thought to be related to greater anticipatory reactivity in the brain [35], it is tempting to speculate that reduced vagal tone and HRV in Npy1r^{rfb} mice might reflect heightened anxiety-related behavior. Following this line of reasoning, reduced expression of Y1Rs on neurons lying in hippocampal areas or their related circuits might account for the imbalance in the autonomic control of resting heart rate that characterizes high levels of anxiety in humans [36] and animal models [37].

In this study, absolute values of HR were similar between mutant and control mice during an acute psychosocial challenge (social defeat). Elevated HR during social defeat was mediated by a decreased vagal tone compared to baseline levels in both groups. However, given that the

concurrent stress-induced increase in HR and decrease in vagal tone were smaller in Npy1r^{rfb} mice, it could be hypothesized that a failure to further decrease cardiac vagal activity contributes to the smaller stress-induced increase in HR in Npy1r^{rfb} mice. Two other factors may account for the reduced HR response to the social challenge in these mutant mice: (i) a somewhat lower level of somatomotor activity, (ii) the fact that HR may have reached its physiological maximum, thus masking the reported differences in baseline HR. Stressful stimuli are processed in multiple limbic forebrain structures, including the amygdala, hippocampus and prefrontal cortex [38]. Limbic stress effector pathways converge on crucial subcortical relay sites, providing for downstream processing of limbic information. In particular, numerous studies link the hippocampus with inhibition of the HPA axis [38, 39]. For example, hippocampal stimulation decreases glucocorticoid secretion in rats and humans [40, 41], whereas hippocampal damage increases stress-induced and in some cases, basal glucocorticoid secretion [39]. Not surprisingly, Npy1r^{rfb} mice show enhanced hypothalamic CRH immunoreactivity and higher serum corticosterone levels [17]. It has been hypothesized that the selective inactivation of Y1Rs in principal excitatory neurons of hippocampus might stimulate HPA axis via the glutamatergic output [17]. Although these limbic circuits are also thought to participate in autonomic integration, their precise role(s) in stress-induced responses is not yet defined. The results of this study provide preliminary evidence that hippocampal Y1R expression might also be involved in the regulation of cardiac autonomic responses to acute stress challenges. On the other hand, no evident differences were observed in HR and HRV parameters in response to the chronic psychosocial challenge employed in this study.

In conclusion, the results of this study provide preliminary evidence that conditional reduction of hippocampal Y1Rs leads to signs of decreased cardiac vagal tone and HRV in mice at rest. On the other hand, the role of hippocampal Y1Rs in the modulation of cardiac autonomic stress response requires deeper investigation. We acknowledge that the robustness of these findings is certainly limited by several factors which need to be addressed in future experiments. For example, Y1R deficiency tied to certain hippocampal (e.g. glutamatergic) neurons might be useful for revealing the precise neurobiological pathways underlying the autonomic phenotype of Npy1r^{rfb} mice. Moreover, Y1R expression should be investigated in other brain areas that may play a role in the

cardiovascular and behavioral effects of hippocampal Y1 receptor deficiency, such as the infralimbic area of the mPFC. Finally, the potential contribution of other phenotypic features of Npy1r^{rfb} mice (such as, reduced body weight, increased anxiety, and increased NPY and CRH content [17]) to the autonomic changes described in this study needs to be taken into account. Nevertheless, this conditional knockout mouse model might be useful for gaining a deeper understanding of the role of Y1Rs in emotional-processing areas of the brain for autonomic nervous system control.

Figure captions

Figure 1. Timeline of the experimental procedures.

Figure 2. Expression of Npy1r mRNA in hippocampal CA1 and CA3 pyramidal cell layers and in the dentate gyrus (DG) granule cell layers in $Npy1r^{rfb}$ mice (n=4) and $Npy1r^{2lox}$ (n=4) mice. Relative optical densities (OD) are expressed as means ± SEM. * indicates a significant difference between $Npy1r^{rfb}$ and $Npy1r^{2lox}$ mice ($p<0.05$).

Figure 3. Time course of changes in heart rate, heart rate variability parameters, body temperature and locomotor activity during the light (L) and the dark (D) phases of baseline daily rhythm recordings, in $Npy1r^{rfb}$ (n = 10) and $Npy1r^{2lox}$ (n = 8) mice. Values are reported as means ± SEM of data obtained by averaging multiple 2 min segments acquired every 30 min for the 12-h light and the 12-h dark phase of the daily cycle. RMSSD = root mean square of successive R-R interval differences; HF = high frequency; LF = low frequency. Statistical results are reported in the results' section.

Figure 4. Time course of changes in heart rate (panels A and B), RMSSD (panels C and D) and high frequency (HF) power (panels E and F) in baseline conditions (bas) and following the injection of vehicle (left panels) or methylscopolamine (right panels) in $Npy1r^{rfb}$ (n = 10) and $Npy1r^{2lox}$ (n = 8) mice. Values are expressed as means ± SEM. * indicates a significant difference between $Npy1r^{rfb}$ and $Npy1r^{2lox}$ mice ($p<0.05$); # indicates a significant difference vs. the respective baseline value ($p<0.05$).

Figure 5. Left panels show the time course of changes in heart rate (A), high frequency (HF) power (C), and locomotor activity (E) values in baseline conditions (bas) and during the first episode of social defeat, in $Npy1r^{rfb}$ (n= 10) and $Npy1r^{2lox}$ (n= 8) mice. Right panels show delta values of heart rate (B), HF power (D), and locomotor activity (F) which were calculated as the difference between

412 mean “fight” and mean baseline values. Absolute and delta values are expressed as means ±

413 SEM. * indicates a significant difference between $Npy1r^{rfb}$ and $Npy1r^{2lox}$ mice ($p<0.05$).

414

Tables

Table 1. Daily rhythms of HR, HRV parameters, body temperature and locomotor activity in baseline condition and during chronic psychosocial stress.

		BASELINE RHYTHMS		STRESS RHYTHMS 1		STRESS RHYTHMS 2	
		Light	Dark	Light	Dark	Light	Dark
HR (bpm)	$Npy1r^{rfb}$	504±7*	567±7*	552±14$^{\#}$	597±15	515±11	582±13
	$Npy1r^{2lox}$	466±12	532±5	533±14$^{\#}$	590±10$^{\#}$	497±11	571±7$^{\#}$
TOTAL power (ms^2)	$Npy1r^{rfb}$	78.7±8.3*	45.2±3.2*	39.3±6.4$^{\#}$	29.0±3.8$^{\#}$	91.9±15.8	41.4±5.6
	$Npy1r^{2lox}$	119.7±14.5	61.4±4.4	51.9±14.1$^{\#}$	28.7±5.6$^{\#}$	87.6±20.6	45.0±7.9
RMSSD (ms)	$Npy1r^{rfb}$	4.6±0.4*	3.2±0.3*	2.7±0.3$^{\#}$	2.3±0.2$^{\#}$	4.6±0.6	3.2±0.4
	$Npy1r^{2lox}$	6.4±0.7	4.2±0.3	3.4±0.8$^{\#}$	2.8±0.4$^{\#}$	4.3±0.7$^{\#}$	3.7±0.7
HF power (ms^2)	$Npy1r^{rfb}$	7.4±1.4*	3.8±0.8	2.6±0.5$^{\#}$	2.1±0.4	7.1±1.7	3.6±0.9
	$Npy1r^{2lox}$	13.4±2.2	5.9±0.8	5.1±2.5$^{\#}$	3.2±0.9$^{\#}$	6.0±1.5$^{\#}$	5.1±1.7
T (°C)	$Npy1r^{rfb}$	36.2±0.2*	37.3±0.2	36.3±0.2	37.2±0.2	36.1±0.2	37.2±0.2
	$Npy1r^{2lox}$	35.8±0.1	37.0±0.1	35.9±0.1	37.0±0.2	35.8±0.1	37.1±0.1
LOC (cpm)	$Npy1r^{rfb}$	4.0±0.4	8.8±1.1	4.4±0.8	11.5±2.3	4.4±0.6	9.4±1.5
	$Npy1r^{2lox}$	4.6±0.5	11.4±1.5	5.2±0.7	12.2±1.7	4.9±0.7	12.4±1.5

Values are reported as mean values ± SEM of data obtained by averaging multiple 2 min segments acquired every 30 min over a 6-day period for baseline rhythms and over a 4-day period for stress rhythms 1 and stress rhythms 2, in $Npy1r^{rfb}$ (n = 10) and $Npy1r^{2lox}$ (n = 8) mice. HR= heart rate; HRV= heart rate variability; RMSSD = root mean square of successive R-R interval differences; HF = high frequency; LF = low frequency; T = body temperature; LOC = locomotor activity. * indicates a significant difference between $Npy1r^{rfb}$ and $Npy1r^{2lox}$ mice; $^{\#}$ indicates a significant difference between stress rhythm value and the respective baseline rhythm value. ($p<0.05$).

429 Acknowledgements

430 This work was supported by the following grants: (i) PRIN2008 PLKP3E_002,_003, and (ii) PRIN

431 2010 7MSMA4_005 and _003 from MIUR to PP and CE.

432

References

[1] Tatemoto K. Neuropeptide Y: history and overview. In: Michel MC, editor. Neuropeptide Y and related peptides. Berlin: Springer; 2004. p. 1-21.

[2] Allen YS, Adrian TE, Allen JM, Tatemoto K, Crow TJ, Bloom SR, et al. Neuropeptide Y distribution in the rat brain. Science. 1983;221:877-9.

[3] Gray TS, Morley JE. Neuropeptide Y: anatomical distribution and possible function in mammalian nervous system. Life Sci. 1986;38:389-401.

[4] Kohler C, Eriksson L, Davies S, Chan-Palay V. Neuropeptide Y innervation of the hippocampal region in the rat and monkey brain. J Comp Neurol. 1986;244:384-400.

[5] Silva AP, Cavadas C, Grouzmann E. Neuropeptide Y and its receptors as potential therapeutic drug targets. Clin Chim Acta. 2002;326:3-25.

[6] Eva C, Serra M, Mele P, Panzica G, Oberto A. Physiology and gene regulation of the brain NPY Y1 receptor. Front Neuroendocrinol. 2006;27:308-39.

[7] Michel MC, Beck-Sickinger A, Cox H, Doods HN, Herzog H, Larhammar D, et al. XVI. International Union of Pharmacology recommendations for the nomenclature of neuropeptide Y, peptide YY, and pancreatic polypeptide receptors. Pharmacol Rev. 1998;50:143-50.

[8] Pedragosa-Badia X, Stichel J, Beck-Sickinger AG. Neuropeptide Y receptors: how to get subtype selectivity. Front Endocrinol. 2013;4:5.

[9] Hastings JA, Pavia JM, Morris MJ. Neuropeptide Y and [Leu31,Pro34]neuropeptide Y potentiate potassium-induced noradrenaline release in the paraventricular nucleus of the aged rat. Brain Res. 1997;750:301-4.

[10] Hastings JA, Morris MJ, Lambert G, Lambert E, Esler M. NPY and NPY Y1 receptor effects on noradrenaline overflow from the rat brain in vitro. Regul Pept. 2004;120:107-12.

[11] Shi YC, Lau J, Lin Z, Zhang H, Zhai L, Sperk G, et al. Arcuate NPY controls sympathetic output and BAT function via a relay of tyrosine hydroxylase neurons in the PVN. Cell Metab. 2013;17:236-48.

[12] Cassaglia PA, Shi Z, Li B, Reis WL, Clute-Reinig NM, Stern JE, et al. Neuropeptide Y acts in the paraventricular nucleus to suppress sympathetic nerve activity and its baroreflex regulation. J Physiol. 2014;592:1655-75.

[13] Tovote P, Meyer M, Beck-Sickinger AG, von Horsten S, Ove Ogren S, Spiess J, et al. Central NPY receptor-mediated alteration of heart rate dynamics in mice during expression of fear conditioned to an auditory cue. Regul Pept. 2004;120:205-14.

[14] Costoli T, Sgoifo A, Stilli D, Flugge G, Adriani W, Laviola G, et al. Behavioural, neural and cardiovascular adaptations in mice lacking the NPY Y1 receptor. Neurosci Biobehav Rev. 2005;29:113-23.

[15] Hirsch D, Zukowska Z. NPY and stress 30 years later: the peripheral view. Cell Mol Neurobiol. 2012;32:645-59.

[16] Sah R, Geracioti TD. Neuropeptide Y and posttraumatic stress disorder. Mol Psychiatry. 2013;18:646-55.

[17] Bertocchi I, Oberto A, Longo A, Mele P, Sabetta M, Bartolomucci A, et al. Regulatory functions of limbic Y1 receptors in body weight and anxiety uncovered by conditional knockout and maternal care. Proc Natl Acad Sci U S A. 2011;108:19395-400.

[18] Costoli T, Bartolomucci A, Graiani G, Stilli D, Laviola G, Sgoifo A. Effects of chronic psychosocial stress on cardiac autonomic responsiveness and myocardial structure in mice. Am J Physiol Heart Circ Physiol. 2004;286:H2133-40.

[19] Bartolomucci A, Palanza P, Gaspani L, Limiroli E, Panerai AE, Ceresini G, et al. Social status in mice: behavioral, endocrine and immune changes are context dependent. Physiol Behav. 2001;73:401-10.

[20] Miczek KA. A new test for aggression in rats without aversive stimulation: differential effects of d-amphetamine and cocaine. Psychopharmacology. 1979;60:253-9.

[21] Thireau J, Zhang BL, Poisson D, Babuty D. Heart rate variability in mice: a theoretical and practical guide. Exp Physiol. 2008;93:83-94.

485 [22] Ramaekers D, Beckers F, Demeulemeester H, Aubert AE. Cardiovascular autonomic function
486 in conscious rats: a novel approach to facilitate stationary conditions. Ann Noninvasive
487 Electrocardiol. 2002;7:307-18.
488 [23] Carnevali L, Trombini M, Porta A, Montano N, de Boer SF, Sgoifo A. Vagal withdrawal and
489 susceptibility to cardiac arrhythmias in rats with high trait aggressiveness. PLoS One.
490 2013;8:e68316.
491 [24] Reyes Del Paso GA, Langewitz W, Mulder LJ, van Roon A, Duschek S. The utility of low
492 frequency heart rate variability as an index of sympathetic cardiac tone: A review with emphasis on
493 a reanalysis of previous studies. Psychophysiology. 2013;50:1183-93.
494 [25] Wisden W, Morris BJ. In situ hybridization with oligonucleotide probes. Int Rev Neurobiol.
495 2002;47:3-59.
496 [26] Bartness TJ, Vaughan CH, Song CK. Sympathetic and sensory innervation of brown adipose
497 tissue. Int J Obes. 2010;34 Suppl 1:S36-42.
498 [27] St-Pierre JA, Nouel D, Dumont Y, Beaudet A, Quirion R. Association of neuropeptide Y Y1
499 receptors with glutamate-positive and NPY-positive neurons in rat hippocampal cultures. Eur J
500 Neurosci. 2000;12:1319-30.
501 [28] Westerhaus MJ, Loewy AD. Central representation of the sympathetic nervous system in the
502 cerebral cortex. Brain Res. 2001;903:117-27.
503 [29] Ruit KG, Neafsey EJ. Hippocampal input to a "visceral motor" corticobulbar pathway: an
504 anatomical and electrophysiological study in the rat. Exp Brain Res. 1990;82:606-16
505 [30] Ruit KG, Neafsey EJ. Cardiovascular and respiratory responses to electrical and chemical
506 stimulation of the hippocampus in anesthetized and awake rats. Brain Res. 1988;457:310-21.
507 [31] Shoemaker JK, Goswami R. Forebrain neurocircuitry associated with human reflex
508 cardiovascular control. Front Physiol. 2015;6:240.
509 [32] Lin EJ, Lin S, Aljanova A, During MJ, Herzog H. Adult-onset hippocampal-specific
510 neuropeptide Y overexpression confers mild anxiolytic effect in mice. Eur Neuropsychopharmacol.
511 2010;20:164-75.

512 [33] Zhou Z, Zhu G, Hariri AR, Enoch MA, Scott D, Sinha R, et al. Genetic variation in human NPY
513 expression affects stress response and emotion. Nature. 2008;452:997-1001.
514 [34] Grillon C. Models and mechanisms of anxiety: evidence from startle studies.
515 Psychopharmacology. 2008;199:421-37.
516 [35] Simmons AN, Stein MB, Strigo IA, Arce E, Hitchcock C, Paulus MP. Anxiety positive subjects
517 show altered processing in the anterior insula during anticipation of negative stimuli. Hum Brain
518 Mapp. 2011;32:1836-46.
519 [36] Pittig A, Arch JJ, Lam CW, Craske MG. Heart rate and heart rate variability in panic, social
520 anxiety, obsessive-compulsive, and generalized anxiety disorders at baseline and in response to
521 relaxation and hyperventilation. Int J Psychophysiol. 2013;87:19-27.
522 [37] Carnevali L, Trombini M, Graiani G, Madeddu D, Quaini F, Landgraf R, et al. Low vagally-
523 mediated heart rate variability and increased susceptibility to ventricular arrhythmias in rats bred
524 for high anxiety. Physiol Behav. 2014;128:16-25.
525 [38] Ulrich-Lai YM, Herman JP. Neural regulation of endocrine and autonomic stress responses.
526 Nat Rev Neurosci. 2009;10:397-409.
527 [39] Herman JP, Figueiredo H, Mueller NK, Ulrich-Lai Y, Ostrander MM, Choi DC, et al. Central
528 mechanisms of stress integration: hierarchical circuitry controlling hypothalamo-pituitary-
529 adrenocortical responsiveness. Front Neuroendocrinol. 2003;24:151-80.
530 [40] Dunn JD, Orr SE. Differential plasma corticosterone responses to hippocampal stimulation.
531 Exp Brain Res. 1984;54:1-6.
532 [41] Rubin RT, Mandell AJ, Crandall PH. Corticosteroid responses to limbic stimulation in man:
533 localization of stimulus sites. Science. 1966;153:767-8.

534

535

Reduced NPY Y1 receptor hippocampal expression and signs of decreased vagal modulation of heart rate in mice

Rosario Statello[1], Luca Carnevali[1], Silvia Paterlini[1], Laura Gioiosa[1], Ilaria Bertocchi[2], Carola Eva[2], Paola Palanza[1*], Andrea Sgoifo[1*].

[1] Department of Neuroscience, University of Parma, Italy

[2] Neuroscience Institute Cavalieri-Ottolenghi Foundation, University of Turin, Italy

Corresponding author: Prof. Andrea Sgoifo, Stress Physiology Laboratory, Department of Neuroscience, University of Parma, Parco Area delle Scienze 11/a, 43123 Parma, Italy

Tel: +39 0521 905625; fax: +39 0521 905673

E-mail address: andrea.sgoifo@unipr.it

* These authors contributed equally to this work

Abstract

Central neuropeptide Y (NPY) signaling participates in the regulation of cardiac autonomic outflow, particularly via activation of NPY-Y1 receptors (Y1Rs). However, the specific brain areas and neural pathways involved have not been completely identified yet. Here, we evaluate the role of hippocampal Y1Rs in the modulation of the autonomic control of cardiac function using a conditional knockout mouse model. Radiotelemetric transmitters were implanted in 4-month-old male mice exhibiting reduced forebrain expression (rfb) of the Y1R ($Npy1r^{rfb}$, n=10) and their corresponding controls ($Npy1r^{2lox}$, n=8). ECG signals were recorded (i) during resting conditions, (ii) under selective pharmacological manipulation of cardiac vagal activity, and (iii) during acute and chronic psychosocial stress challenges, and analyzed via time- and frequency-domain analysis of heart rate variability. $Npy1r^{rfb}$ mice showed a lower Npy1r mRNA density in the dentate gyrus and in the CA1 region of the hippocampus. Under resting undisturbed conditions, $Npy1r^{rfb}$ mice exhibited (i) a higher heart rate, (ii) a reduced overall heart rate variability, and (iii) lower values of the indices of vagal modulation compared to $Npy1r^{2lox}$ counterparts. Following pharmacological vagal inhibition, heart rate was higher in control but not in $Npy1r^{rfb}$ mice compared to their respective baseline values, suggesting that tonic vagal influences on heart rate were reduced in $Npy1r^{rfb}$ mice. The magnitude of the heart rate response to an acute psychosocial stressor was smaller in $Npy1r^{rfb}$ mice compared to $Npy1r^{2lox}$ counterparts (likely due to a concurrent lower vagal withdrawal), even though absolute heart rate values did not differ between the two groups. These findings suggest that reduced hippocampal Y1R expression leads to a decrease in resting vagal modulation and heart rate variability, which, in turn, may determine a reduced cardiac autonomic responsiveness to acute stress challenges.

Keywords: NPY; Stress; Heart; Autonomic; knockout; Parasympathetic.

1. Introduction

Neuropeptide Y (NPY) is widely distributed in the central nervous system [1], with particularly high concentrations in the hypothalamus [2] and limbic system [3, 4]. NPY is involved in the regulation of a variety of complex functions that range from food intake to emotional state [5]. These effects are mediated by multiple G-protein coupled receptor subtypes, which are characterized by different tissue localization and pharmacological properties [6-8]. In particular, accumulating evidence suggests that central Y1 receptors (Y1Rs) play a critical role in the inhibition of the sympathetic outflow to peripheral tissues. For example, it has been shown in rats that i.c.v. (lateral ventricle) administration of the Y1R agonist [Leu^{31},Pro^{34}]NPY reduces basal noradrenaline release from the paraventricular nucleus of the hypothalamus (PVN) [9], the major site of autonomic regulation via projections to the rostral ventro-lateral medulla and the spinal cord. Moreover, NPY, acting on Y1Rs, decreases noradrenaline overflow from both the hypothalamus and the medulla in vitro [10]. A recent study has elegantly demonstrated that NPY released from the arcuate nucleus (ARC) suppresses tyrosine hydroxylase (TH) expression in the PVN via activation of Y1Rs [11]. This effect was associated with a reduction in TH expression in the locus coeruleus and other regions (such as the A1/C1 cell groups) in the brain stem [11], which would ultimately lead to a reduced sympathetic outflow to peripheral tissues [11]. Supporting this view, nanoinjection of NPY into the PVN decreases heart rate (HR), sympathetic nerve activity and baroreflex control of HR in anesthetized rats via activation of Y1Rs and Y5Rs [12]. In mice, Tovote and colleagues observed that bilateral i.c.v. injections of NPY dose-dependently induced bradycardia and also blunted the tachycardic response to a fear conditioning challenge [13], the latter via Y1R-mediated inhibition of stress-induced sympathetic activation [13]. Similarly, global knockout of the Y1 receptor gene in mice led to a larger HR activation during social defeat stress [14]. These findings support the view that NPY-Y1R signaling may play an important role also in constraining stress-induced sympathetic activation [15, 16]. While the relationship between NPY-Y1R signaling in the ARC/PVN axis and sympathetic nervous system has been documented, there is little known about the neural pathways and mechanisms that control it. Indeed, in contrast with the above reported observations that are suggestive of a central sympathetic inhibitory role of Y1Rs, global knockout of the NPY-

Y1R gene in mice led to resting bradycardia, which was likely due to a reduced basal sympathetic tone and increased parasympathetic activity [14]. This apparent contradiction might be ascribed to compensatory effects that are due to gene inactivation in early development and/or might underlie different roles played by Y1Rs at different levels in the central autonomic network.

Recently, a conditional knockout mouse model in which the inactivation of the Y1 receptor gene is restricted to excitatory neurons in the hippocampus, in particular when mice were reared by foster mothers exhibiting high levels of maternal care, has been developed [17]. Therefore, this animal model may be useful for understanding the contribution of hippocampal Y1Rs for central autonomic cardiovascular control. In order to reach this goal, autonomic modulation of cardiac function was assessed in the above mentioned conditional knockout mouse model during (i) baseline conditions, (ii) selective pharmacological autonomic manipulations, and (iii) acute and chronic psychosocial stress challenges, via time- and frequency-domain analysis of HR variability (HRV).

2. Methods

2.1. Animals, housing conditions and ethics statements

Experiments were performed on 4-month-old male conditional knockout mice ($Npy1r^{rfb}$, n=10) and their control littermates ($Npy1r^{2lox}$, n=8) that were matched for body weight. $Npy1r^{rfb}$ and $Npy1r^{2lox}$ mice (background strain: C57BL/6J) were generated following the breeding scheme described by Bertocchi et al. (see [17] for details). Briefly, $Npy1r^{2lox}/Tg^{\alpha CamKII\text{-}tTA/LC1}$ mice (named herein $Npy1r^{rfb}$) were generated using doxycycline dependent control of the Cre-LoxP system. Using this approach, Bertocchi et al. [17] achieved the deletion of Npy1r in the hippocampal CA1 and CA3 pyramidal and in the dentate gyrus granule cell layers. Since the phenotype of $Npy1r^{rfb}$ mutants becomes evident only in males reared by foster mothers showing high level of maternal cares versus adopted pups, immediately after birth the $Npy1r^{rfb}$ male mice used in our study were fostered to Dox-naive CD1 dams, which display high levels of maternal cares (unpublished data). Littermates comprising $Npy1r^{2lox}/Tg^{\alpha CamKII\text{-}tTA}$, $Npy1^{r2lox}/Tg^{LC1}$, and $Npy1r^{2lox}$ genotypes were used as controls (named herein $Npy1r^{2lox}$ controls), as in Bertocchi et al. [17]. After weaning, mice were kept in same sex sibling groups in 40x20x20 cages in rooms with humidity- (50 ± 10%) and temperature- (22 ± 2 °C) controlled conditions, with food and water available ad libitum. Experiments were performed during the light phase of the 12-h light/dark cycle (lights on at 7 a.m.). All experimental procedures and protocols were approved by the Veterinarian Animal Care and Use Committee of Parma University and conducted in accordance with the European Community Council Directives of 22 September 2010 (2010/63/UE).

2.2. Transmitter implantation and radiotelemetry system

ECG (sampling frequency 2 KHz), body temperature (T, °C) and locomotor activity (LOC, counts per minute, cpm) signals were recorded by a radiotelemetry system. It consisted of transmitters (TA10ETA-F20, Data Sciences Int., St.Paul, MN, USA) and platform receivers (RPC-1, Data Science Int., St.Paul, MN, USA), which were connected to a computer containing Art-Gold 1.10 data acquisition system (Data Science Int., St.Paul, MN, USA). Transmitter implantation was performed under isoflurane anesthesia (2% in 100% oxygen), as previously described [18]. The

transmitter's body was implanted intraperitoneally and two electrodes (wire loops) were fixed to the dorsal surface of the xyphoid process and in the anterior mediastinum close to the right atrium, respectively. This surgical procedure guarantees high quality ECG recordings, even during sustained physical activity. After surgery, mice were individually housed, injected with Gentamicin sulphate (Aagent, Fatro, 1ml/kg, S.C.) and allowed two weeks of recovery before the beginning of the experimental recordings.

2.3. General experimental outline

The timeline of the experimental protocol is depicted in Figure 1. Specific experimental procedures and data analysis are described in the following sections. After recovery from surgery, mice were weighed and left undisturbed in their home cages for 6 days (days 1-6). On days 7 and 9, they underwent pharmacological autonomic challenges. From day 12 to day 25, mice were housed in the cage of a dominant mouse in order to mimic a chronic psychosocial stress condition. At the end of the experimental protocol, mice were sacrificed by decapitation. Brains were rapidly removed and immediately frozen in liquid nitrogen, then stored at -80° C until analysis.

2.4. Daily rhythms of HR, HRV, T and LOC

ECG, T and LOC signals were sampled around-the-clock for 2 min every 30 min in baseline conditions (Basal Rhythms, days 1-6) and during chronic psychosocial stress (Stress Rhythms 1, days 16-19; Stress Rhythms 2, days 22-25) (Fig. 1). Heart rate (HR, beats per minute, bpm), HRV parameters (see ECG analysis section for details), T and LOC were calculated as mean values of the 12-h light and 12-h dark phases of the daily cycle for each recording day. Subsequently, they were further averaged as mean values of the light and dark phase for each recording period.

2.5. Pharmacological autonomic challenge

On day 7 and 9 (Fig. 1), mice were intraperitoneally injected with either i) vehicle (0.9% NaCl, 1 ml/kg) or ii) methylscopolamine (muscarinic receptor antagonist, 0.1 mg/kg), with a rotational

151 design. Continuous ECG recordings were performed prior to (for 30 min, baseline condition) and
152 following (for 60 min) each injection, with the mice in their home cages.
153
154 2.6. Chronic psychosocial stress
155 In the present study we applied a modified version of the standard chronic psychosocial stress
156 paradigm [18, 19], which is based on the classical resident-intruder test [20]. Six-month-old CD1
157 mice were housed with a female partner for 1 week and then individually housed and trained to
158 aggressively defend their territory from same sex mice intruders that were younger and lighter.
159 These dominant animals served as residents. Each experimental mouse was introduced as an
160 intruder in the home cage of a resident male; once there, it was attacked and subordinated by the
161 resident mouse (social defeat). After 10 min, the two animals were separated by a perforated
162 polystyrene-metal partition that divided the cage into two equal-area sections. Thus, the intruder
163 mouse was protected from direct physical contact but it was in constant olfactory, auditory and
164 visual contact with the resident (psychosocial challenge). The partition was removed five times
165 during the experimental protocol (Fig. 1) at an unpredictable time between 9:00 and 13:00 h and
166 repositioned after 2 min to prevent injuries. After each interaction, the experimental mice were
167 closely inspected for any improper injury and were excluded from further procedures in case they
168 were wounded. During the first episode of agonistic interaction, continuous ECG recordings were
169 performed for 30 min in baseline conditions (with the mice in their home cage), during the 10-min
170 agonistic interaction, and for 60 min after the intruders were again separated from the residents by
171 the partition.
172
173 2.7. Heart rate variability (HRV) analysis
174 HRV analysis was carried out on ECG recordings using ChartPro 5.0 software (ADInstrument,
175 Sydney, Australia), based on the recommendations for HRV analysis in mice [21]. Initially, each
176 ECG recording was split in 2-min temporal segments (0-2 min; 2-4 min; etc.). Ectopic beats and
177 recording artifacts were then removed following visual inspection of unprocessed ECG signals.
178 Subsequently, HR and time- and frequency-domain parameters of HRV were quantified for each 2-

min time period. In the time domain, the root mean square of successive R-R interval differences (RMSSD, ms) was quantified; this index reflects short-term, high-frequency variations of RR interval, which are mainly due to cardiac parasympathetic activity [22]. In the frequency-domain, the power spectrum was obtained with a fast Fourier transform-based method (Welch's periodogram: 256 points, 50% overlap, and Hamming window). The following parameters were evaluated: i) the total power of the spectrum (ms^2), which reflects all the cyclic components responsible for variability [23], and ii) the power (ms^2) of the high frequency band (HF, 1.5-5.0 Hz), which reflects the activity of the parasympathetic nervous system and is related to respiratory sinus arrhythmia [24].

2.8. In Situ Hybridization for Npy1r mRNA

In situ hybridization was performed on 14-µm-thick coronal brain sections, according to the protocol reported by Wisden and Morris [25], in $Npy1r^{rfb}$ (n=4) and $Npy1r^{2lox}$ (n=4) mice. Four different 40-/45-mer oligonucleotide S35-labeled probes were simultaneously used to increase the signal and the reaction was carried out as previously described [17]. The area of interest of clearly distinguishable nuclei was defined following the boundaries of the labeled regions [dentate gyrus granule cell layer (DG)], whereas three to four spots were used for each slice in poorly contrasted regions [CA1 pyramidal cell layer (CA1) and CA3 pyramidal cell layer (CA3)]. Optical densities (OD unit) were measured and averaged after a rodboard calibration. Background was measured by averaging three to five spots in the surrounding blank region of the autoradiogram, then subtracted from the corresponding nucleus value.

.

2.9. Statistical analysis

All statistical analyses were performed using the software package SPSS (version 22). Two-way ANOVA for repeated measures with "group" as between-subject factor (2 levels: $Npy1r^{rfb}$ and $Npy1r^{2lox}$) was applied for ECG and telemetric data obtained from: i) baseline around-the-clock recordings, with "time" as within-subject factor (6 levels: day 1, 2, 3, 4, 5 and 6); ii) pharmacological challenges, with "time" as within-subject factor (4 levels: baseline; post injection 1, 2, 3); iii) first

episode of social defeat, with “time” as within-subject factor (8 levels: baseline, fight, sensory contact 1, 2, 3, 4, 5 and 6); iv) around-the-clock recordings during chronic social stress, with “time” as within-subject factor (3 levels: baseline, stress 1 and stress 2). Follow-up analyses were conducted using Student’s “t” tests, with a Bonferroni correction for multiple comparisons for each outcome variable separately. Statistical significance was set at $p<0.05$.

213 # 3. Results

214

215 ## 3.1. Body weight

216 Prior to surgery, body weight was 25.0±0.9 g for Npy1r^{rfb} mice and 26.0±1.2 g for Npy1r^{2lox} mice
217 (n.s.). No significant differences between the two groups were found in body weight at the
218 beginning of the experimental protocol (day 1) (Npy1r^{rfb}: 26.3±0.3 g vs. Npy1r^{2lox} 27.2±0.8 g).

219

220 ## 3.2. Expression of Npy1r mRNA in the hippocampus of control and conditional mutants

221 In Npy1r^{rfb} mice, Npy1r mRNA expression was significantly lower in hippocampal CA1 pyramidal
222 cell layers ($t=-3.1$, $p<0.05$) and in dentate gyrus granule cell layers ($t=-3.4$, $p<0.05$) compared with
223 their control littermates, whereas no difference was observed in CA3 pyramidal cell layers between
224 the two groups (Fig. 2).

225

226 ## 3.3. Daily rhythms of HR, HRV, T and LOC during baseline conditions

227 The daily rhythms of HR, HRV indices, T and LOC in resting conditions are depicted in Figure 3
228 and summarized in Table 1. Two-way ANOVA yielded a main effect of "group" for HR ($F=20.1$,
229 $p<0.01$), total power ($F=7.0$, $p<0.05$), RMSSD ($F=5.3$, $p<0.05$), and HF ($F=4.6$, $p<0.05$) values.
230 Follow-up analyses revealed that Npy1r^{rfb} mice had significantly higher HR values than Npy1r^{2lox}
231 mice during both the light ($t=2.9$, $p<0.05$) and dark ($t=3.9$, $p<0.01$) phases of the daily cycle (Fig.
232 3A and Table 1). Npy1r^{rfb} mice exhibited significantly lower values of total power than Npy1r^{2lox}
233 mice during both the light ($t=2.6$, $p<0.05$) and the dark ($t=3.0$, $p<0.01$) phases of the light-dark
234 cycle (Fig. 3B and Table 1). RMSSD values also resulted significantly lower in Npy1r^{rfb} mice than
235 Npy1r^{2lox} counterparts in both phases (light: $t=2.4$, $p<0.05$; dark: $t=2.5$, $p<0.05$) (Fig. 3C and Table
236 1). Also spectral power values in the HF band were lower in Npy1r^{rfb} compared to Npy1r^{2lox} mice
237 (light: $t=2.4$, $p<0.05$; dark: $t=1.9$, $p=0.07$) (Fig. 3D and Table 1). In addition, Npy1r^{rfb} mice had
238 significantly higher T values than Npy1r^{2lox} mice during the light phase ($t=2.0$, $p=0.05$) (Fig. 3E and
239 Table 1). Lastly, no significant differences between the two groups were observed for LOC values
240 (Fig. 3F and Table 1).

241

242 3.4. Cardiac autonomic response to the pharmacological autonomic manipulation

243 Cardiac autonomic responses to vehicle or methylscopolamine injection are depicted in Figure 4.

244 Before vehicle injection, HR was significantly higher in Npy1r^{rfb} than in Npy1r^{2lox} mice (t=2.6,

245 p<0.05) (Fig. 4A). In the same period, HRV analysis revealed that Npy1r^{rfb} mice had significantly

246 lower values of RMSSD (t=2.1, p=0.05) and HF spectral power (t=2.2, p<0.05) compared to

247 Npy1r^{2lox} mice (Fig. 4C, E). The injection of vehicle provoked an increase in HR and a reduction in

248 RMSSD and HF values in both groups, with no group differences in the mean values of these

249 parameters (Fig. 4A, C, E). All parameters returned to baseline values within 40 min. During the

250 last 20-min recording period (min 40-60), mean HR was significantly higher in Npy1r^{rfb} compared to

251 Npy1r^{2lox} mice (t=2.2, p<0.05) (Fig. 4A). In the same period, RMSSD and HF mean values were

252 lower in Npy1r^{rfb} than in Npy1r^{2lox} mice (RMSSD: t=2.0, p=0.06; HF: t=2.6, p<0.05) (Fig. 4C, E).

253 Before methylscopolamine injection, HR was significantly higher in Npy1r^{rfb} compared to Npy1r^{2lox}

254 mice (t=2.3, p<0.05). Blockade of muscarinic receptors with methylscopolamine provoked a

255 significant reduction of RMSSD (Npy1r^{rfb}: t=8.5, p<0.01; Npy1r^{2lox}: t=6.5, p<0.01) and HF (Npy1r^{rfb}:

256 t=5.4, p<0.01; Npy1r^{2lox}: t=4.1, p<0.01) values in both groups that persisted through the 60-min

257 recording period (Fig. 4D, F). There were no differences in the peak HR response to

258 methylscopolamine injection between the two groups (Fig. 4B). However, contrary to what has

259 been observed during vehicle (control) condition, during the last 20-min recording period (min 40-

260 60) mean HR was (i) similar between the two groups, and (ii) significantly higher in Npy1r^{2lox}

261 compared to the respective baseline value (t=2.2, p<0.05).

262

263 3.5. HR, HRV, and LOC response to the first episode of social defeat

264 Cardiac autonomic and LOC responses to the first episode of social defeat are depicted in Figure

265 5. Two-way ANOVA yielded a significant effect of time for HR (F=18.9, p<0.01) and LOC (F=4.4,

266 p<0.05) values. In baseline conditions, HR was significantly higher in Npy1r^{rfb} than in Npy1r^{2lox}

267 mice (t=2.2, p<0.05) (Fig. 5A). No differences in absolute values of HR were observed between the

268 two groups during the 10-min fight period and the following 60-min sensory contact phase (Fig.

5A). However, the magnitude of the HR response during the 10-min fight period (delta values) was significantly smaller in Npy1r^{rfb} than in Npy1r^{2lox} mice (t=-4.6, p<0.01) (Fig. 5B). Consistently, in baseline conditions Npy1r^{rfb} mice had significantly lower HF spectral power values compared with Npy1r^{2lox} mice (t=2.5, p<0.05) (Fig. 5C). During the 10-min fight period, HF absolute values were similar between the two groups (Fig. 5C), with the magnitude of the stress-induced reduction in HF values being significantly smaller in Npy1r^{rfb} than in Npy1r^{2lox} mice (t=2.5, p<0.05) (Fig. 5D). No differences in LOC values were observed between Npy1r^{rfb} and Npy1r^{2lox} mice in baseline conditions and in response to the social challenge (Fig. 5E, F).

3.6. Daily rhythms of HR, HRV, T and LOC during chronic psychosocial stress

HR, HRV, T and LOC values during the light and dark phases of the chronic psychosocial stress period are summarized in Table1. Two-way ANOVA revealed that chronic exposure to psychosocial stress led to (i) higher HR values (F_{light}=20.0, p<0.01; F_{dark}=19.8, p<0.01), and (ii) lower RMSSD (F_{light}=4.9, p<0.05), total power (F_{dark}=7.2, p<0.05) and HF (F_{light}=6.7, p<0.05) values compared to baseline conditions (Table 1). However, there were no differences between the two groups in HR, HRV parameters, T and LOC during both stress rhythm 1 and stress rhythm 2 periods (Table 1).

4. Discussion

This study demonstrates that reduced expression of hippocampal Y1Rs in mice is associated with an increase in heart rate and a decrease in vagal neural modulation at rest.

In the present study, HRV analysis was carried out in order to characterize cardiac autonomic neural modulation of Npy1r^{rfb} mice under different experimental conditions. During both the light and the dark phases of the daily cycle, Npy1r^{rfb} mice exhibited a lower cardiac vagal modulation, as indexed by RMSSD and HF, which was likely responsible for the resting tachycardia and reduced overall HRV (total power) observed in these mice. Indeed, such changes could not be ascribed to a different level of somatomotor activity between the two groups. Rather, an important confirmation of the involvement of autonomic mechanisms in determining resting tachycardia in Npy1r^{rfb} mice comes from the pharmacological blockade of muscarinic receptors with methylscopolamine. Under this condition of potent and sustained pharmacological inhibition of cardiac vagal modulation, and after recovery from the stress of injection (see vehicle injection condition for a comparison), the group difference in baseline heart rate was abolished. This was due to the fact that heart rate under pharmacological vagal inhibition was higher in control but not in Npy1r^{rfb} mice compared to their respective baseline values. Consequently, it may be reasonable to hypothesize that tonic vagal influences on heart rate were reduced in Npy1r^{rfb} mice, leading to resting tachycardia. Interestingly, we found that baseline body temperature values were also somewhat higher in Npy1r^{rfb} mice. In rodents, brown adipose tissue (BAT) is the main site of nonshivering thermogenesis, and it is under tight control by the sympathetic nervous system [26]. Therefore, signs of hyperthermia in Npy1r^{rfb} mice might suggest an increased sympathetic drive to BAT.

In this study, Npy1r^{rfb} mice Y1R expression is significantly reduced in the dentate gyrus and the CA1 region of the hippocampus, where Y1Rs have been associated with glutamate-positive and NPY-positive neurons [27]. The ventral CA1 hippocampal field is thought to be linked by multisynaptic connections to the sympathetic-related regions of the hypothalamus, suggesting its possible involvement in a higher-brain autonomic circuit [28]. In addition, the hippocampus

connects to nucleus tractus solitarius-projecting regions of the medial prefrontal cortex (mPFC), such as the infralimbic cortex [29], indicating that hippocampal actions on autonomic function may also be routed through the mPFC. Importantly, electrical and chemical stimulation of the hippocampal formation in the anesthetized and the awake rat decreases heart rate, blood pressure and respiratory rate [30, 31]. Interestingly, pharmacological manipulation of vagal activity with methylatropine revealed that the cardiovascular, but not the respiratory, responses were mediated partially by vagal influences and partially by sympathetic influences [30]. Taken together, these preliminary observations indicate that hippocampal Y1Rs may participate in the control of autonomic outflow to peripheral tissues under baseline, undisturbed conditions. In a previous study, Npy1r^{rfb} mice have been characterized as having reduced body weight, less adipose tissue, and lower serum leptin levels [17]. Here, mice did not differ for body weight, either prior or after surgery recovery, as they were matched to avoid possible bias. Therefore, we might cautiously assume that body weight is not a major determinant of the autonomic phenotype described in Npy1r^{rfb} mice. On the other hand, the hippocampus is an important component of the neuronal circuitry controlling anxiety-related behaviors and Npy1r^{rfb} mice have been previously shown to display higher levels of anxiety in the elevated plus maze and open field tests [17]. These findings are consistent with a previous observation that overexpression of virally-transduced NPY in the mouse hippocampus produces anxiolytic-like effects [32]. Moreover, in humans NPY haploinsufficiency is correlated with trait anxiety [33]. Given that anticipation of future aversive events is a key aspect of anxiety disorders [34] and that anxiety is thought to be related to greater anticipatory reactivity in the brain [35], it is tempting to speculate that reduced vagal tone and HRV in Npy1r^{rfb} mice might reflect heightened anxiety-related behavior. Following this line of reasoning, reduced expression of Y1Rs on neurons lying in hippocampal areas or their related circuits might account for the imbalance in the autonomic control of resting heart rate that characterizes high levels of anxiety in humans [36] and animal models [37].

In this study, absolute values of HR were similar between mutant and control mice during an acute psychosocial challenge (social defeat). Elevated HR during social defeat was mediated by a decreased vagal tone compared to baseline levels in both groups. However, given that the

concurrent stress-induced increase in HR and decrease in vagal tone were smaller in Npy1r^{rfb} mice, it could be hypothesized that a failure to further decrease cardiac vagal activity contributes to the smaller stress-induced increase in HR in Npy1r^{rfb} mice. Two other factors may account for the reduced HR response to the social challenge in these mutant mice: (i) a somewhat lower level of somatomotor activity, (ii) the fact that HR may have reached its physiological maximum, thus masking the reported differences in baseline HR. Stressful stimuli are processed in multiple limbic forebrain structures, including the amygdala, hippocampus and prefrontal cortex [38]. Limbic stress effector pathways converge on crucial subcortical relay sites, providing for downstream processing of limbic information. In particular, numerous studies link the hippocampus with inhibition of the HPA axis [38, 39]. For example, hippocampal stimulation decreases glucocorticoid secretion in rats and humans [40, 41], whereas hippocampal damage increases stress-induced and in some cases, basal glucocorticoid secretion [39]. Not surprisingly, Npy1r^{rfb} mice show enhanced hypothalamic CRH immunoreactivity and higher serum corticosterone levels [17]. It has been hypothesized that the selective inactivation of Y1Rs in principal excitatory neurons of hippocampus might stimulate HPA axis via the glutamatergic output [17]. Although these limbic circuits are also thought to participate in autonomic integration, their precise role(s) in stress-induced responses is not yet defined. The results of this study provide preliminary evidence that hippocampal Y1R expression might also be involved in the regulation of cardiac autonomic responses to acute stress challenges. On the other hand, no evident differences were observed in HR and HRV parameters in response to the chronic psychosocial challenge employed in this study.

In conclusion, the results of this study provide preliminary evidence that conditional reduction of hippocampal Y1Rs leads to signs of decreased cardiac vagal tone and HRV in mice at rest. On the other hand, the role of hippocampal Y1Rs in the modulation of cardiac autonomic stress response requires deeper investigation. We acknowledge that the robustness of these findings is certainly limited by several factors which need to be addressed in future experiments. For example, Y1R deficiency tied to certain hippocampal (e.g. glutamatergic) neurons might be useful for revealing the precise neurobiological pathways underlying the autonomic phenotype of Npy1r^{rfb} mice. Moreover, Y1R expression should be investigated in other brain areas that may play a role in the

cardiovascular and behavioral effects of hippocampal Y1 receptor deficiency, such as the infralimbic area of the mPFC. Finally, the potential contribution of other phenotypic features of $Npy1r^{rfb}$ mice (such as, reduced body weight, increased anxiety, and increased NPY and CRH content [17]) to the autonomic changes described in this study needs to be taken into account. Nevertheless, this conditional knockout mouse model might be useful for gaining a deeper understanding of the role of Y1Rs in emotional-processing areas of the brain for autonomic nervous system control.

Figure captions

Figure 1. Timeline of the experimental procedures.

Figure 2. Expression of Npy1r mRNA in hippocampal CA1 and CA3 pyramidal cell layers and in the dentate gyrus (DG) granule cell layers in $Npy1r^{rfb}$ mice (n=4) and $Npy1r^{2lox}$ (n=4) mice. Relative optical densities (OD) are expressed as means ± SEM. * indicates a significant difference between $Npy1r^{rfb}$ and $Npy1r^{2lox}$ mice ($p<0.05$).

Figure 3. Time course of changes in heart rate, heart rate variability parameters, body temperature and locomotor activity during the light (L) and the dark (D) phases of baseline daily rhythm recordings, in $Npy1r^{rfb}$ (n = 10) and $Npy1r^{2lox}$ (n = 8) mice. Values are reported as means ± SEM of data obtained by averaging multiple 2 min segments acquired every 30 min for the 12-h light and the 12-h dark phase of the daily cycle. RMSSD = root mean square of successive R-R interval differences; HF = high frequency; LF = low frequency. Statistical results are reported in the results' section.

Figure 4. Time course of changes in heart rate (panels A and B), RMSSD (panels C and D) and high frequency (HF) power (panels E and F) in baseline conditions (bas) and following the injection of vehicle (left panels) or methylscopolamine (right panels) in $Npy1r^{rfb}$ (n = 10) and $Npy1r^{2lox}$ (n = 8) mice. Values are expressed as means ± SEM. * indicates a significant difference between $Npy1r^{rfb}$ and $Npy1r^{2lox}$ mice ($p<0.05$); # indicates a significant difference vs. the respective baseline value ($p<0.05$).

Figure 5. Left panels show the time course of changes in heart rate (A), high frequency (HF) power (C), and locomotor activity (E) values in baseline conditions (bas) and during the first episode of social defeat, in $Npy1r^{rfb}$ (n= 10) and $Npy1r^{2lox}$ (n= 8) mice. Right panels show delta values of heart rate (B), HF power (D), and locomotor activity (F) which were calculated as the difference between

412 mean “fight” and mean baseline values. Absolute and delta values are expressed as means ±
413 SEM. * indicates a significant difference between $Npy1r^{rfb}$ and $Npy1r^{2lox}$ mice ($p<0.05$).
414

Tables

Table 1. Daily rhythms of HR, HRV parameters, body temperature and locomotor activity in baseline condition and during chronic psychosocial stress.

		BASELINE RHYTHMS		STRESS RHYTHMS 1		STRESS RHYTHMS 2	
		Light	Dark	Light	Dark	Light	Dark
HR (bpm)	$Npy1r^{rfb}$	504±7*	567±7*	552±14$^{\#}$	597±15	515±11	582±13
	$Npy1r^{2lox}$	466±12	532±5	533±14$^{\#}$	590±10$^{\#}$	497±11	571±7$^{\#}$
TOTAL power (ms^2)	$Npy1r^{rfb}$	78.7±8.3*	45.2±3.2*	39.3±6.4$^{\#}$	29.0±3.8$^{\#}$	91.9±15.8	41.4±5.6
	$Npy1r^{2lox}$	119.7±14.5	61.4±4.4	51.9±14.1$^{\#}$	28.7±5.6$^{\#}$	87.6±20.6	45.0±7.9
RMSSD (ms)	$Npy1r^{rfb}$	4.6±0.4*	3.2±0.3*	2.7±0.3$^{\#}$	2.3±0.2$^{\#}$	4.6±0.6	3.2±0.4
	$Npy1r^{2lox}$	6.4±0.7	4.2±0.3	3.4±0.8$^{\#}$	2.8±0.4$^{\#}$	4.3±0.7$^{\#}$	3.7±0.7
HF power (ms^2)	$Npy1r^{rfb}$	7.4±1.4*	3.8±0.8	2.6±0.5$^{\#}$	2.1±0.4	7.1±1.7	3.6±0.9
	$Npy1r^{2lox}$	13.4±2.2	5.9±0.8	5.1±2.5$^{\#}$	3.2±0.9$^{\#}$	6.0±1.5$^{\#}$	5.1±1.7
T (°C)	$Npy1r^{rfb}$	36.2±0.2*	37.3±0.2	36.3±0.2	37.2±0.2	36.1±0.2	37.2±0.2
	$Npy1r^{2lox}$	35.8±0.1	37.0±0.1	35.9±0.1	37.0±0.2	35.8±0.1	37.1±0.1
LOC (cpm)	$Npy1r^{rfb}$	4.0±0.4	8.8±1.1	4.4±0.8	11.5±2.3	4.4±0.6	9.4±1.5
	$Npy1r^{2lox}$	4.6±0.5	11.4±1.5	5.2±0.7	12.2±1.7	4.9±0.7	12.4±1.5

Values are reported as mean values ± SEM of data obtained by averaging multiple 2 min segments acquired every 30 min over a 6-day period for baseline rhythms and over a 4-day period for stress rhythms 1 and stress rhythms 2, in $Npy1r^{rfb}$ (n = 10) and $Npy1r^{2lox}$ (n = 8) mice. HR= heart rate; HRV= heart rate variability; RMSSD = root mean square of successive R-R interval differences; HF = high frequency; LF = low frequency; T = body temperature; LOC = locomotor activity. * indicates a significant difference between $Npy1r^{rfb}$ and $Npy1r^{2lox}$ mice; $^{\#}$ indicates a significant difference between stress rhythm value and the respective baseline rhythm value. ($p<0.05$).

429 Acknowledgements

430 This work was supported by the following grants: (i) PRIN2008 PLKP3E_002,_003, and (ii) PRIN

431 2010 7MSMA4_005 and _003 from MIUR to PP and CE.

432

References

[1] Tatemoto K. Neuropeptide Y: history and overview. In: Michel MC, editor. Neuropeptide Y and related peptides. Berlin: Springer; 2004. p. 1-21.

[2] Allen YS, Adrian TE, Allen JM, Tatemoto K, Crow TJ, Bloom SR, et al. Neuropeptide Y distribution in the rat brain. Science. 1983;221:877-9.

[3] Gray TS, Morley JE. Neuropeptide Y: anatomical distribution and possible function in mammalian nervous system. Life Sci. 1986;38:389-401.

[4] Kohler C, Eriksson L, Davies S, Chan-Palay V. Neuropeptide Y innervation of the hippocampal region in the rat and monkey brain. J Comp Neurol. 1986;244:384-400.

[5] Silva AP, Cavadas C, Grouzmann E. Neuropeptide Y and its receptors as potential therapeutic drug targets. Clin Chim Acta. 2002;326:3-25.

[6] Eva C, Serra M, Mele P, Panzica G, Oberto A. Physiology and gene regulation of the brain NPY Y1 receptor. Front Neuroendocrinol. 2006;27:308-39.

[7] Michel MC, Beck-Sickinger A, Cox H, Doods HN, Herzog H, Larhammar D, et al. XVI. International Union of Pharmacology recommendations for the nomenclature of neuropeptide Y, peptide YY, and pancreatic polypeptide receptors. Pharmacol Rev. 1998;50:143-50.

[8] Pedragosa-Badia X, Stichel J, Beck-Sickinger AG. Neuropeptide Y receptors: how to get subtype selectivity. Front Endocrinol. 2013;4:5.

[9] Hastings JA, Pavia JM, Morris MJ. Neuropeptide Y and [Leu31,Pro34]neuropeptide Y potentiate potassium-induced noradrenaline release in the paraventricular nucleus of the aged rat. Brain Res. 1997;750:301-4.

[10] Hastings JA, Morris MJ, Lambert G, Lambert E, Esler M. NPY and NPY Y1 receptor effects on noradrenaline overflow from the rat brain in vitro. Regul Pept. 2004;120:107-12.

[11] Shi YC, Lau J, Lin Z, Zhang H, Zhai L, Sperk G, et al. Arcuate NPY controls sympathetic output and BAT function via a relay of tyrosine hydroxylase neurons in the PVN. Cell Metab. 2013;17:236-48.

[12] Cassaglia PA, Shi Z, Li B, Reis WL, Clute-Reinig NM, Stern JE, et al. Neuropeptide Y acts in the paraventricular nucleus to suppress sympathetic nerve activity and its baroreflex regulation. J Physiol. 2014;592:1655-75.

[13] Tovote P, Meyer M, Beck-Sickinger AG, von Horsten S, Ove Ogren S, Spiess J, et al. Central NPY receptor-mediated alteration of heart rate dynamics in mice during expression of fear conditioned to an auditory cue. Regul Pept. 2004;120:205-14.

[14] Costoli T, Sgoifo A, Stilli D, Flugge G, Adriani W, Laviola G, et al. Behavioural, neural and cardiovascular adaptations in mice lacking the NPY Y1 receptor. Neurosci Biobehav Rev. 2005;29:113-23.

[15] Hirsch D, Zukowska Z. NPY and stress 30 years later: the peripheral view. Cell Mol Neurobiol. 2012;32:645-59.

[16] Sah R, Geracioti TD. Neuropeptide Y and posttraumatic stress disorder. Mol Psychiatry. 2013;18:646-55.

[17] Bertocchi I, Oberto A, Longo A, Mele P, Sabetta M, Bartolomucci A, et al. Regulatory functions of limbic Y1 receptors in body weight and anxiety uncovered by conditional knockout and maternal care. Proc Natl Acad Sci U S A. 2011;108:19395-400.

[18] Costoli T, Bartolomucci A, Graiani G, Stilli D, Laviola G, Sgoifo A. Effects of chronic psychosocial stress on cardiac autonomic responsiveness and myocardial structure in mice. Am J Physiol Heart Circ Physiol. 2004;286:H2133-40.

[19] Bartolomucci A, Palanza P, Gaspani L, Limiroli E, Panerai AE, Ceresini G, et al. Social status in mice: behavioral, endocrine and immune changes are context dependent. Physiol Behav. 2001;73:401-10.

[20] Miczek KA. A new test for aggression in rats without aversive stimulation: differential effects of d-amphetamine and cocaine. Psychopharmacology. 1979;60:253-9.

[21] Thireau J, Zhang BL, Poisson D, Babuty D. Heart rate variability in mice: a theoretical and practical guide. Exp Physiol. 2008;93:83-94.

485 [22] Ramaekers D, Beckers F, Demeulemeester H, Aubert AE. Cardiovascular autonomic function
486 in conscious rats: a novel approach to facilitate stationary conditions. Ann Noninvasive
487 Electrocardiol. 2002;7:307-18.
488 [23] Carnevali L, Trombini M, Porta A, Montano N, de Boer SF, Sgoifo A. Vagal withdrawal and
489 susceptibility to cardiac arrhythmias in rats with high trait aggressiveness. PLoS One.
490 2013;8:e68316.
491 [24] Reyes Del Paso GA, Langewitz W, Mulder LJ, van Roon A, Duschek S. The utility of low
492 frequency heart rate variability as an index of sympathetic cardiac tone: A review with emphasis on
493 a reanalysis of previous studies. Psychophysiology. 2013;50:1183-93.
494 [25] Wisden W, Morris BJ. In situ hybridization with oligonucleotide probes. Int Rev Neurobiol.
495 2002;47:3-59.
496 [26] Bartness TJ, Vaughan CH, Song CK. Sympathetic and sensory innervation of brown adipose
497 tissue. Int J Obes. 2010;34 Suppl 1:S36-42.
498 [27] St-Pierre JA, Nouel D, Dumont Y, Beaudet A, Quirion R. Association of neuropeptide Y Y1
499 receptors with glutamate-positive and NPY-positive neurons in rat hippocampal cultures. Eur J
500 Neurosci. 2000;12:1319-30.
501 [28] Westerhaus MJ, Loewy AD. Central representation of the sympathetic nervous system in the
502 cerebral cortex. Brain Res. 2001;903:117-27.
503 [29] Ruit KG, Neafsey EJ. Hippocampal input to a "visceral motor" corticobulbar pathway: an
504 anatomical and electrophysiological study in the rat. Exp Brain Res. 1990;82:606-16
505 [30] Ruit KG, Neafsey EJ. Cardiovascular and respiratory responses to electrical and chemical
506 stimulation of the hippocampus in anesthetized and awake rats. Brain Res. 1988;457:310-21.
507 [31] Shoemaker JK, Goswami R. Forebrain neurocircuitry associated with human reflex
508 cardiovascular control. Front Physiol. 2015;6:240.
509 [32] Lin EJ, Lin S, Aljanova A, During MJ, Herzog H. Adult-onset hippocampal-specific
510 neuropeptide Y overexpression confers mild anxiolytic effect in mice. Eur Neuropsychopharmacol.
511 2010;20:164-75.

512 [33] Zhou Z, Zhu G, Hariri AR, Enoch MA, Scott D, Sinha R, et al. Genetic variation in human NPY
513 expression affects stress response and emotion. Nature. 2008;452:997-1001.
514 [34] Grillon C. Models and mechanisms of anxiety: evidence from startle studies.
515 Psychopharmacology. 2008;199:421-37.
516 [35] Simmons AN, Stein MB, Strigo IA, Arce E, Hitchcock C, Paulus MP. Anxiety positive subjects
517 show altered processing in the anterior insula during anticipation of negative stimuli. Hum Brain
518 Mapp. 2011;32:1836-46.
519 [36] Pittig A, Arch JJ, Lam CW, Craske MG. Heart rate and heart rate variability in panic, social
520 anxiety, obsessive-compulsive, and generalized anxiety disorders at baseline and in response to
521 relaxation and hyperventilation. Int J Psychophysiol. 2013;87:19-27.
522 [37] Carnevali L, Trombini M, Graiani G, Madeddu D, Quaini F, Landgraf R, et al. Low vagally-
523 mediated heart rate variability and increased susceptibility to ventricular arrhythmias in rats bred
524 for high anxiety. Physiol Behav. 2014;128:16-25.
525 [38] Ulrich-Lai YM, Herman JP. Neural regulation of endocrine and autonomic stress responses.
526 Nat Rev Neurosci. 2009;10:397-409.
527 [39] Herman JP, Figueiredo H, Mueller NK, Ulrich-Lai Y, Ostrander MM, Choi DC, et al. Central
528 mechanisms of stress integration: hierarchical circuitry controlling hypothalamo-pituitary-
529 adrenocortical responsiveness. Front Neuroendocrinol. 2003;24:151-80.
530 [40] Dunn JD, Orr SE. Differential plasma corticosterone responses to hippocampal stimulation.
531 Exp Brain Res. 1984;54:1-6.
532 [41] Rubin RT, Mandell AJ, Crandall PH. Corticosteroid responses to limbic stimulation in man:
533 localization of stimulus sites. Science. 1966;153:767-8.

534

535

Figure 1

Click here to download high resolution image

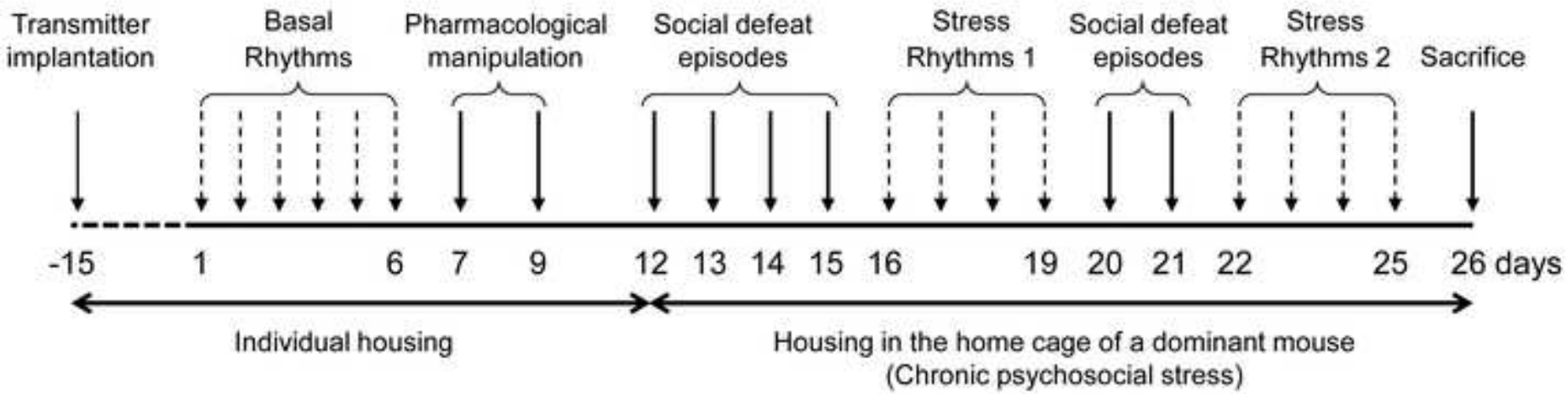

Figure 2
Click here to download high resolution image

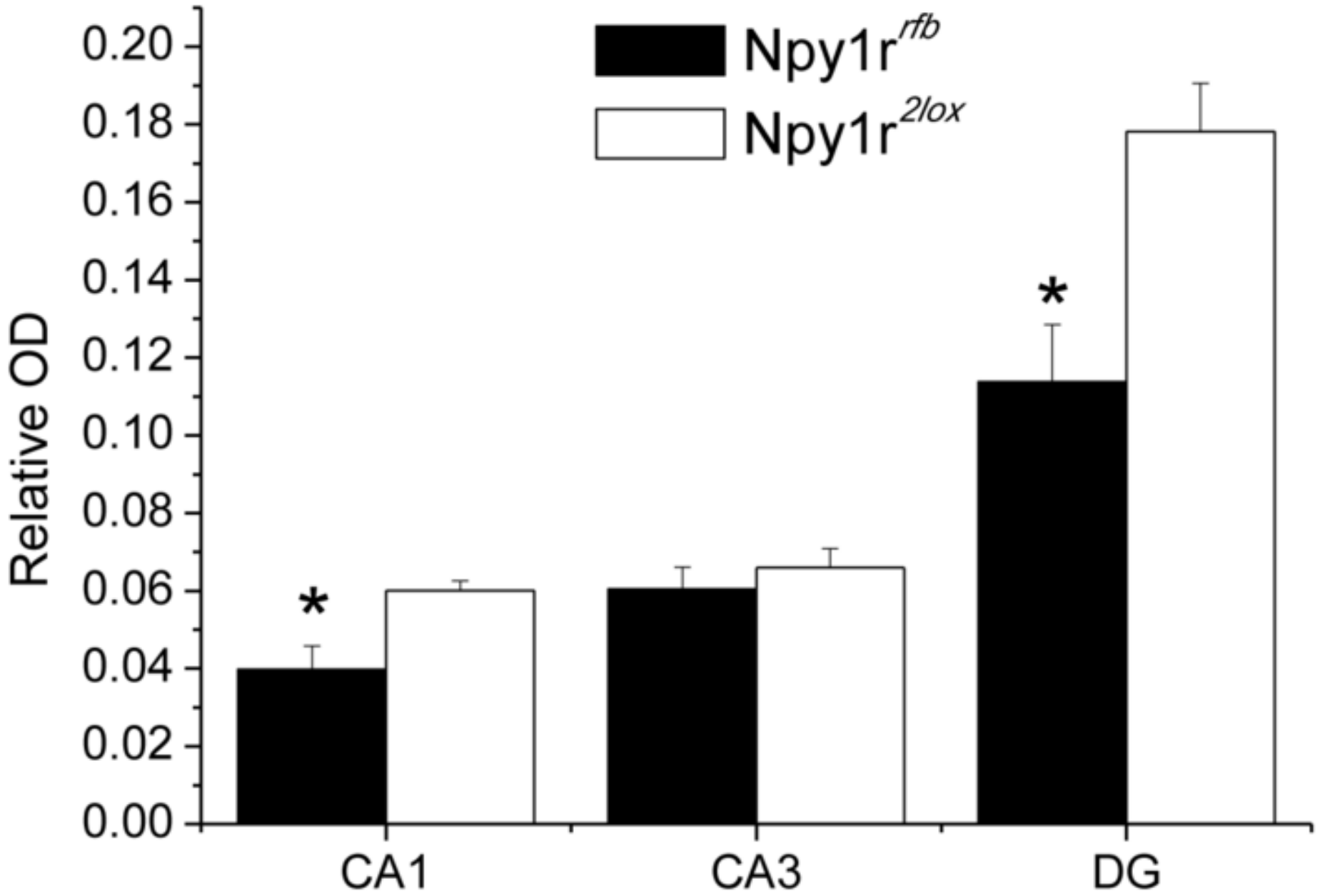

Figure 3
Click here to download high resolution image

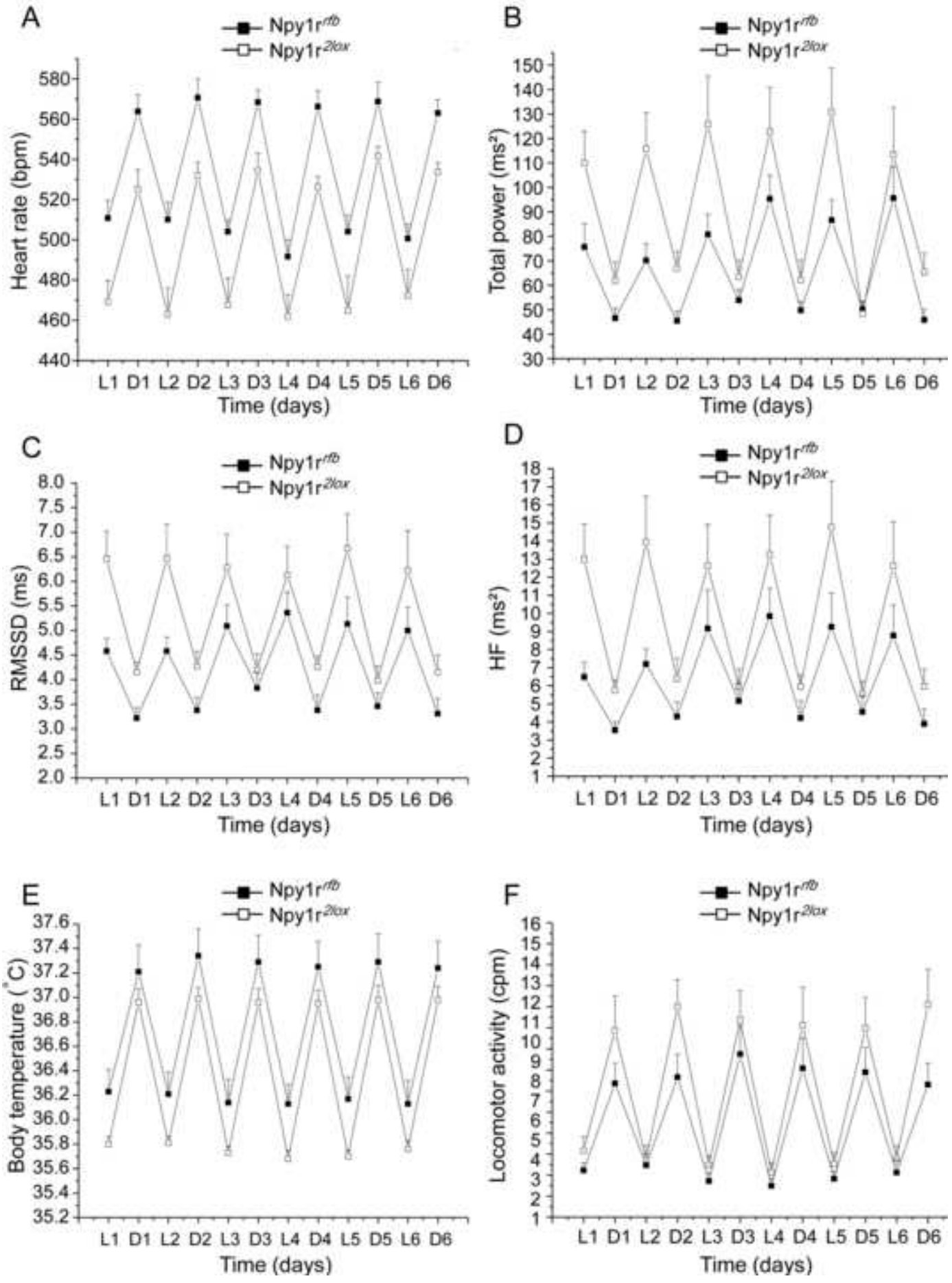

Figure 4
Click here to download high resolution image

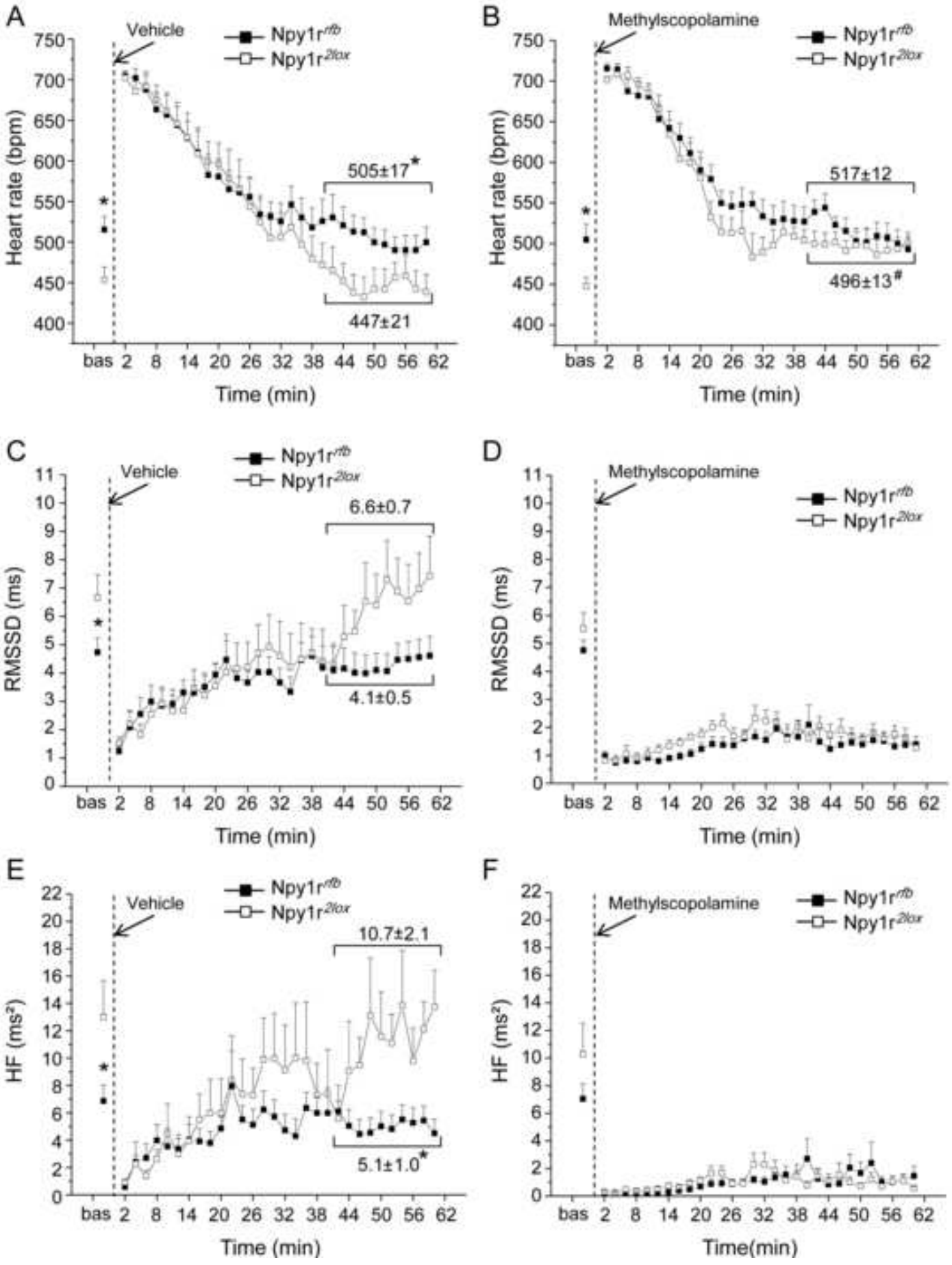

Figure 5
Click here to download high resolution image